Published in final edited form as:
Pflugers Arch. 2010 September ; 460(4): 767–776. doi:10.1007/s00424-010-0839-8.

Ryanodol action on calcium sparks in ventricular myocytes

Josefina Ramos-Franco, **Ana M. Gomez**[*], **Alma Nani**, **Yiwei Liu**, **Julio A. Copello**[†], and **Michael Fill**
Rush University Medical Center Department of Molecular Biophysics & Physiology 1750 West Harrison Street Chicago, IL 60612 USA

[*]INSERM U-637 CHU A. de Villeneuve Montpellier 34295 FRANCE

[†]Southern Illinois University Department of Pharmacology 801 N Rutledge Street Springfield, IL 62794, USA

Abstract

The action of ryanodol on single cardiac ryanodine receptor (RyR2) channels in bilayers and local RyR2-mediated Ca^{2+} release events (Ca^{2+} sparks) in ventricular myocytes was defined. At the single channel level, ryanodol intermittently modified single channels into a long lived sub-conductance state with an average duration of 3.8±0.2 s. Unlike ryanodine, ryanodol did not change the open probability (Po) of unmodified channels and high concentrations did not promote full channel closure. Ryanodol action was Po dependent with the K_D varying roughly from 20 to 80 μM as Po changed from ~0.2 to 1, respectively. Ryanodol preferentially bound during long channel openings. In intact and permeabilized rat myocytes, ryanodol evoked trains of sparks at active release sites resulting in a significant increase in overall spark frequency. Ryanodol did not increase the number of active release sites. Long lived Ca^{2+} release events were observed but infrequently and ryanodol action was readily reversed upon drug washout. We propose that ryanodol modifies a few channels during a Ca^{2+} spark. These modified channels mediate a sustained low intensity Ca^{2+} release that repeatedly triggers sparks at the same release site. We conclude that ryanodol is an easily generated reversible probe that can be effectively used to explore RyR2-mediated Ca^{2+} release in cells.

INTRODUCTION

In cardiac muscle, a small trans-sarcolemma Ca^{2+} influx through voltage-dependent Ca^{2+} channels activates the type-2 RyR channel (RyR2) which releases Ca^{2+} from the sarcoplasmic reticulum (SR). This process is commonly called Ca^{2+}-induced Ca^{2+} release (CICR). In cells, the RyR2 channels are clustered at discrete sites on the SR and the concerted Ca^{2+} release at such a site generates the Ca^{2+} spark [8, 11, 13, 27, 28]. The summation of Ca^{2+} sparks is thought to generate the global intracellular Ca^{2+} signals that normally control contractility [17].

Numerous endogenous and exogenous agents are known to alter RyR2 function [3]. The most specific pharmacological probe is ryanodine, a plant alkaloid that binds with nanomolar affinity to the channel. The dissociation rate constant of ryanodine is quite slow [41] and thus ryanodine can take hours to fall off its binding site. This makes its action essentially irreversible during the time frame (~30 minutes) of a typical single channel or Ca^{2+} spark experiment [44, 31]. At the single channel level, 1–10 μM ryanodine locks the

Electronic supplementary material The online version of this article (doi:10.1007/s00424-010-0839-8) contains supplementary material, which is available to authorized users.

channel into a long-lived subconductance state [17]. Ryanodine-modified RyR channels in cells generate prolonged low intensity local Ca^{2+} release events called embers or glows [22, 44]. Low doses of ryanodine (e.g. 50 nM) do not immediately generate visible embers but instead evoke repeated activations at individual Ca^{2+} spark sites [34]. Consecutive sparks at the same site has become an important means to explore spark restitution and refractoriness [12–14, 34].

Alterations in the chemical structure of ryanodine have produced many different types of ryanoids that compete with ryanodine at a common binding site [42, 4, 23]. The affinity and effective reversibility of these ryanoids varies widely. There are relatively few studies that have explored the actions of these other ryanoids in muscle cells [22] and none to our knowledge in cardiac muscle. This is probably because these agents are not commercially available. A simple method for converting ryanodine into ryanodol was described 50 years ago [24] but is rarely utilized today. Here, we used this classic method to generate high purity ryanodol and explored its efficacy at both the single channel and cellular levels. Like low dose ryanodine, ryanodol evoked repeated Ca^{2+} sparks at individual release sites. Unlike ryanodine, ryanodol appears to act via a simple bimolecular reaction and its effects are reversible making it an interesting probe to explore Ca^{2+} spark regulatory mechanisms.

MATERIAL AND METHODS

Microsome Preparation

SR microsomes were isolated from the ventricular muscle of adult rat hearts using standard procedures [9]. Briefly, the tissue was rinsed in a saline solution (154 mM NaCl, 10 mM Tris-malate, pH 6.8) at a temperature of 4°C before being chopped and homogenized. A heavy microsomal fraction was then isolated from the homogenate by differential centrifugation on a discontinuous sucrose gradient. The SR microsomal fractions were collected and diluted into a saline solution containing 300 mM sucrose. These samples were then flash frozen and stored at −80°C until used.

Single Channel Studies

Planar lipid bilayers were formed across a 100 μm hole in a thin (~12 μm) teflon partition separating two aqueous compartments. Bilayers were made from a mixture (50 mg/ml in decane) of phosphatidylethanolamine (PE), phosphatidylserine (PS) and phosphatidylcholine (PC) in a 5:4:1 ratio. Lipids were obtained from Avanti Polar Lipids (Pelham, AL). Microsomes were added to one compartment that was defined as cytosolic because the cytosolic side of the RyR2 channel will be in this solution [40]. The other compartment was defined as luminal. The cytosolic compartment was virtually grounded and filled with a HEPES-Tris solution (250 mM / 120 mM) at pH 7.4. The luminal compartment was filled with HEPES-Ca^{2+} (250 mM / 50 mM), pH 7.4. Experiments were done at room temperature (~21°C). Unless otherwise specified, salts and chemicals were obtained from Sigma Chemical Company (St. Louis, MO) or Calbiochem (San Diego, CA).

The free Ca^{2+} concentration in the cytosolic solution was buffered using BAPTA and/or dibromoBAPTA. Free Ca^{2+} concentration was calculated with the MaxChelator program (WinMaxC Stanford University, CA) and verified using a Ca^{2+}-selective microelectrodes prepare as described previously [1]. The Ca^{2+}, ATP and caffeine concentration in the cytosolic chamber was varied. Membrane voltage was controlled using a patch-clamp amplifier (Axopatch 200B; Axon Instruments, Union City, CA). Unitary (single channel) currents represent net Ca^{2+} current in the lumen-to-cytosol direction. The current signal was digitized at 10 kHz and subsequently filtered at 1 kHz unless specified otherwise. Data

acquisition and analysis were carried out using pClamp software (Axon instruments, Union City, CA). The holding potential in all experiments was 20 mV.

The % modification (%MOD) was determined from single channel recordings as the relative time spent in the ryanodol-evoked sub-conductance state. The %MOD was evaluated using the following equation (equation 1).

$$\%MOD = \%MOD_{MAX}\left(\frac{[Ryanodol]^N}{K^N + [Ryanodol]^N}\right)$$

The parameters K and N represent the apparent dissociation constant (K_D) and the Hill coefficient. The ryanodol-RyR interaction was assumed to be a simple bimolecular reaction [35] described using the following equation (equation 2).

$$K_D = \frac{k_{OFF}\left(s^{-1}\right)}{k_{ON}\left(\mu M^{-1} \cdot s^{-1}\right)}$$

where k_{OFF} and k_{ON} represent the apparent dissociation and association rate constants.

Sparks Studies

Ventricular myocytes were obtained from adult male Wistar rats (250-300 g) using standard procedures as previously described [2]. Isolated cells were then loaded with the membrane permeant Ca^{2+} dye Fluo-3 AM [19]. These loaded intact myocytes were then perfused with a Tyrode solution containing (in mM): 140 NaCl, 1.1 $MgCl_2$, 1.8 $CaCl_2$, 4 KCl, 10 glucose and 10 HEPES. The pH of this solution was adjusted to 7.4 with NaOH. Cells were then field stimulated at 1 Hz for 1–2 minutes using two parallel platinum electrodes. Field stimulation was applied to check cell excitability as well as allow a stable SR Ca^{2+} load to be achieved. After field stimulation, Ca^{2+} sparks were recorded over a 30 s period with and without ryanodol present. Caffeine (10 mM) was then rapidly applied to empty the SR Ca^{2+} stores. The amplitude of the caffeine evoked Ca^{2+} release was used to assess the global SR Ca^{2+} load.

For other studies, following the loading protocol, isolated cells were permeabilized by a 60s exposure to 0.01% saponin [29]. Saponin was dissolved in an internal solution containing (in mM); 120 L-aspartic acid, 10 HEPES, 0.5 EGTA, 3 MgATP, 10 sodium phosphocreatine and 5 units/ml creatine phosphokinase. The pH of this solution was adjusted to 7.2 with KOH. After permeabilization, the cells were perfused with the same intracellular solution (without saponin) containing Fluo-3 (30 μM pentapotassium salt; Tefflabs) and enough $CaCl_2$ to achieve a free Ca^{2+} concentration of 100 nM. Again, peak caffeine (20 mM) evoked Ca^{2+} release was used to assess the global SR Ca^{2+} load.

Loaded intact and permeabilized cells were imaged using a scanning confocal microscope (Zeiss LSM 510) and a water immersion objective (x63, 1.2 numerical aperture). Fluo-3 fluorescence was excited by 488nm light from an argon ion laser. Emitted light was measured at wavelengths ≥ 515 nm. Line-scan images were obtained at 1.5 ms per line along the longitudinal axis of the cell. An automated Ca^{2+} spark detection and analysis routine (IDL software) based on that of Cheng et al. [10] was used. This routine is like that used recently elsewhere [16, 20, 30]. The spark detection threshold used here was 3.5 standard deviations from the resting fluorescence. Nevertheless, small amplitude sparks are likely underrepresented in our spark amplitude histograms (i.e. lost in the noise). All

experiments were done at 21°C and carried out within 7 hours of cell isolation. Summary results are reported as mean±SEM with significance ($p<0.001$) indicated as determined by unpaired Student's T tests. Lastly, the terms local and global are applied here as described by Cheng and Lederer [12]. Briefly, local events (e.g. sparks) are those that occur at the level of a single SR Ca^{2+} release unit or dyad. Global events (e.g. Ca^{2+} transients) are those that occur cell-wide and represent the spatiotemporal summation of numerous local events.

Ryanodol Preparation

Following a suggestion made by Dr. John Sutko (University of Nevada), we generated ryanodol following the method originally described by Jenden and Fairhurst [24]. Specifically, commercially available ryanodine (purity: ≥*98% by HPLC*; Calbiochem, San Diego, CA) was dissolved in a small volume of NaOH (500 mM). This solution was then placed in a 95°C water bath for ~120 minutes. It was then diluted to a final ryanoid concentration of 10 mM with a HEPES (~60 mM) solution. The pH of the resulting ryanodol stock solution was then adjusted to pH 7.4 using HCl. The reproducibility of this process was verified by generating 3 different ryanodine samples that were tested separately in single RyR channel studies. No difference in efficacy and affinity between samples was detected.

The saponization process described above generates equal molar amounts of ryanodol and the pyrrole ring. Thus, our ryanodol stock contains the pyrrole ring and possibly some contaminant ryanodine. Large concentrations of the pyrrole ring do not alter RyR permeation or gating (see Fig. 1B). Mass spectrometry measurements, performed by Carbon Dynamics (Springfield, IL), measured the amount of ryanodine in 1 mM ryanodol samples (n=3, each from a different preparation). The average level of ryanodine in these samples was 0.000897 mM indicating the samples were >99.9% ryanodol. This number implies that there could be up to 1 nM contaminant ryanodine present for every μM ryanodol applied in our studies. Note that 5–50 nM ryanodine increases the Po of single RyR channels [6, 7] and higher doses evoke an effectively irreversible modification of the channel [7]. However, no evidence of such ryanodine actions were observed in either our single channel or cellular studies. Sigalas et al. [33] also used this type of ryanodol generation method and concluded that it had completely converted ryanodine to ryanodol.

RESULTS

Figure 1A shows spontaneous steady state single RyR2 channel activity in the presence of 10 μM cytosolic free Ca^{2+}. All these channel recordings are from the same channel. Before ryanodol application (top), the channel fluctuated frequently between the full open and closed states. Addition of 40 μM ryanodol to the cytosolic side of the channel evoked intermittent sojourns to a long lived sub-conductance state (middle), the ryanodol-modified state. This action of ryanodol was eliminated upon washout of the added ryanodol (bottom). The same washout experiment done with ryanodine did not eliminate/reverse the ryanodine-modified state within the time frame of the experiment (not shown).

The ryanoid backbone structure is shown in Figure 1B. The ryanoid is ryanodine when the X group is a pyrrole ring (pyrrole-2-carboxylic acid). It is ryanodol when the X group is a hydroxyl. Saponization of ryanodine (see methods) detaches the pyrrole ring at the 3-carbon generating ryanodol [4; 24]. Our ryanodol stock solutions contain the detached pyrrole ring. Figure 1B shows that 100 and 200 μM of the pyrrole ring alone, pyrrole-2-carboxylic acid (99% pure; Sigma-Adrich, St. Louis, MO), did not change Po or alter the unit current of the channel. The mean Po's (n=3) were 0.89±0.07, 0.93±0.04 and 0.85±0.05 for control, 100 and 200 μM pyrrole ring, respectively. The mean current amplitudes here were 5.95±0.24, 5.96±0.13 and 5.83±0.36. The mean open times were 13.54±9.41, 10.60±5.95, and

9.29±6.15. The mean closed times were 0.47±0.10, 0.42±0.05, and 0.53±0.04, respectively. Similar negative results were obtained when pyrrole was added to channels at a low Po level (not shown).

Like others [37], we noted that the noise level of the ryanodol modified subconductance state was greater than that of the fully open state. Generally, a noisy sub-conductance can be characteristic of a fast "flicker" blockade [43]. In Figure 1C, recordings in control and 40 μM ryanodol are shown. The control (c1) and top ryanodol recording (r1) were filtered at 1 kHz. The same ryanodol recording filtered at 2, 3 or 4 kHz (r2, r3 & r4) are shown below. The corresponding all-points histograms are shown (Fig. 1C, right). The peak labeled "r1" reflects the ryanodol-evoked long-lived sub-conductance filtered at 1 kHz and it is centered at ~3 pA in this example. Reduced filtering broadened this peak but did not shift it indicating that the reduced conductance was not likely due to a simple "flicker" block mechanism.

Figure 2 illustrates the concentration dependence of ryanodol action on single RyR2 channels. In Figure 2A, ryanodol evoked sojourns to the modified state and the frequency of these sojourns increased with ryanodol concentration. This ryanodol action was observed regardless of whether ryanodol was added to the cytosolic or luminal solutions indicating that ryanodol can access its site of action from either side of the membrane. The percentage of time a channel spends in the modified state was measured over a wide range of ryanodol concentrations and these results are summarized in Figure 2B. These data were fit by Equation 1 and revealed an apparent K_D of 46.4 ± 6.0 μM with a cooperativity coefficient of 0.91. The histograms in Figure 2C show the durations of individual sojourns in the modified and unmodified states when 40 μM ryanodol was present. Each histogram was fit by a single exponential revealing a ryanodol dissociation rate of 0.32 s^{-1} and an association rate of 8.13×10^{-3} $\mu M^{-1}ms^{-1}$. Plugging these rates into Equation 2 indicates a K_D of 39.5 μM suggesting that the ryanodol-channel interaction is fairly well described by a simple bimolecular reaction. In the absence of ryanodol (control), mean unit Ca^{2+} current carried by single RyR2 channels was 6.08 ± 0.01 pA (n=10). Mean unit Ca^{2+} current carried by an unmodified RyR2 channel in the presence of 40 μM ryanodol was 6.14 ± 0.01 pA (n=9). Mean unit Ca^{2+} current of the ryanodol modified channel was 2.91 ± 0.11 pA (n=9) or ~47% that of the unmodified channel. This is quite consistent to the ryanodol actions previously reported [26, 33, 36, 38].

Ryanodine binding is Po dependent and this is why it can be used to probe the functional status of the RyR channel (14). To determine if ryanodol binding is also Po dependent, a standard ryanodol dose (40 μM) was applied to single RyR2 channels that were activated to different extents by different pharmacological agents. Channels were activated by cytosolic Ca^{2+} (1, 5 & 10 μM), ATP (0.5, 1 or 2 mM) or caffeine (5 mM). Sample recordings of Ca^{2+} and caffeine activated channels are shown in Figure 2D before (control) and after ryanodol addition. When the control Po level was low (top recording), 40 μM ryanodol evoked few sojourns to the modified state. When the control Po level was higher (lower recordings), 40 μM ryanodol evoked much more frequent sojourns to the modified state. Figure 2E shows how the mean ryanodol modification duration (top), % modification and apparent affinity vary with Po. The Po here was determined during unmodified periods (ryanodol present). The average duration of ryanodol-induced modifications over entire Po range was 3.8±0.2 seconds (n=14). Average modification duration at Po's <0.25 and >0.75 was 3.5±0.4 seconds (n=4) and 4.0±0.4 seconds (n=4), respectively. These later two values are not significantly different (T-test; p>0.40). There was a tight positive correlation (R=0.95) between % modification and Po. This relationship did not appear to depend on how the RyR2 channel was activated. Circles, triangles and squares reflect channels activated by Ca^{2+}, ATP and caffeine, respectively. There also appears to be a linear relationship between K_D and Po. To

determine K_D here, the ryanodol association and dissociation rates were determined as shown in Figure 2C and then input into equation 2. The change in K_D was due to the Po sensitivity of the association rate. The dissociation rate was Po independent.

Low doses of ryanodine (i.e. concentrations near the K_D of ryanodine binding) increase the Po of single RyR channels without evoking the long lived subconductance state [6, 7, 34]. To determine if ryanodol does the same, we measured Po during unmodified periods with 40 μM ryanodol present. The mean Po's during unmodified periods (ryanodol present) were 0.03±0.02, 0.54±0.24 and 0.65±0.16 with 1, 5 and 10 μM cytosolic Ca^{2+} present, respectively. The corresponding paired Po's determined in the same cytosolic Ca^{2+} levels with no ryanodol present were 0.02±0.02, 0.59±0.09 and 0.69±0.14, respectively. The presence of ryanodol did not significantly alter the Po of the unmodified channel as expected if there was virtually no ryanodine in our ryanodol samples.

Figure 3A shows that the Po sensitivity of ryanodol action stems from preferential ryanodol binding to the open configuration of the channel. Numerous individual ryanodol modifications were collected (n=385 from 22 different channels). Each was classified into one of four different categories (O-M-O, C-M-C, O-M-C and C-M-O). The O-M-O indicates the modification (M) started and ended from/to the full open state (O). The C-M-C indicates the modification started and ended from/to the closed state (C). The O-M-C indicates the modification started from O state and ended to the C state. The C-M-O indicates the modification started from C state and ended to the O state. For this analysis, the average unmodified Po was kept constant at 0.5 so that likelihood of the channel being open or closed were equal. If ryanodol binding is independent of channel open status, then the probability of a modification falling into any one of the categories would be 0.25 (dashed line). However, the probability of a ryanodol modification falling into the O-M-O category was almost unity while the probability of falling in any of the other categories was nearly zero. This suggests that ryanodol preferentially binds to and unbinds from open channels.

If this is true, then ryanodol modifications should occur more often during long openings. Traditional open dwell time analysis was done in the presence of 5 μM Ca^{2+} (Fig. 3B left), 1 mM ATP (Fig. 3B middle) and 5 mM caffeine (Fig. 3B right). We measured open times of full conductance openings during unmodified periods with 40 μM ryanodol present. The result was the traditional open time histograms shown and these were fit assuming the presence of 2 exponential components (long and short). Then, the mean open time of the full conductance opening just prior to the ryanodol modifications (MOT_M) was determined. Note that the start of a ryanodol modification marked the end of these full conductance openings. For each experimental condition, the average MOT_M (circle) is superimposed on the corresponding dwell time histograms. Ryanodol modifications were preferentially associated with long open events.

The diastolic cytosolic free Ca^{2+} concentration in cardiac myocytes is ~100 nM [3] and consequently RyR2 channel Po in a resting cell is normally very low and mean open time very short [17]. One exception to this is during a Ca^{2+} spark. During the spark, local RyR2 Po is momentarily high and mean open times substantially longer than usual. Thus, the likelihood of ryanodol binding should be greatest during a spark. We explored ryanodol action on sparks in both intact and permeabilized ventricular myocytes. Figure 4A shows action of 10 μM ryanodine on sparks in saponin-permeabilized myocytes. The fluorescence profile at the marked site (arrow) is shown below the line scan image. The spark shown is followed by a long low intensity ember or glow. This is the expected action of 10 μM ryanodine [44, 22, 21, 32, 25]. Figures 4B and 4C shows sample line scan images recorded in a permeabilized cell before (control) and after 50 μM ryanodol was applied. Again, fluorescence profiles are show below the images. In the absence of ryanodol, typical spark

activity was observed (Fig. 4B). After exposure to ryanodol (Fig. 4C), sparks were on average smaller and frequently repeated at individual release sites. This action was observed nearly instantaneously (in <10s) after ryanodine application. Figure 4D summarizes the average Ca^{2+} spark amplitude before (Ctrl) and after ryanodol (Ry) treatment. Figure 4E shows spark amplitude histograms before and after ryanodol treatment. These histograms were fit by the sum of two log-normal distributions. Figure 4F shows how ryanodol changed spark frequency and illustrates that the ryanodol action can be readily reversed after the ryanodol is washout of the solution bathing these permeabilized cells.

Figure 5A shows Ca^{2+} sparks in intact cardiac myocytes before and after addition of 50 μM ryanodol. Within 3 minutes of the ryanodol application, ryanodol significantly increased the overall frequency of Ca^{2+} sparks and evoked repeated sparks at the same site. This action was sustained while ryanodol was present. Figure 5B shows that the mean Ca^{2+} spark frequency after ryanodol application was significantly increased. Interestingly, the number of release sites in the cell generating Ca^{2+} sparks was not changed by the presence of ryanodol (Fig. 5C). Ryanodol increased overall spark frequency by significantly increasing the probability of repeating sparks (spark trains) at individual release sites (Fig. 5D). Figures 5E, 5F and 5G show that ryanodol also significantly reduced the average spark amplitude, decay time constant and spatial half width of sparks in these intact cells. Reduced spark amplitude, spark decay time constant and half width would be a logical consequence of fewer RyR2 channels participating in the spark [12]. It could also be due to a decrease in SR Ca^{2+} load. To access the global Ca^{2+} load, we measured the peak caffeine (10 mM) evoked Ca^{2+} release (Fig. 5H) in the absence and presence of ryanodol. Ryanodol did not significantly change the global SR Ca^{2+} load (5.71±0.5 vs. 5.3 ± 0.5 F/F_0, respectively; n=9). Ryanodol also did not significantly change electrically stimulated cell shortening or the global electrically stimulated Ca^{2+} transient amplitude, decay time or time to peak (see supplementary material). Note that the local load was not measured in this study.

DISCUSSION

A simple long-known chemical treatment of ryanodine [24] was applied here to generate ryanodol. The ryanodol generated was >99.9% pure and had the expected action on single RyR2 channels. It also also evoked repeated Ca^{2+} sparks at individual release sites in mammalian cardiac ventricular myocytes. To our knowledge, this is the first report of ryanodol action on sparks in cardiac muscle. Its reversibility and ease of generated it make ryanodol an attractive alternative to using ryanodine in isolated RyR channel and spark studies.

Ryanodol Action on Single RyR2 Channels

Ryanodol intermittently modified RyR2 channels into a long lived subconductance state. The mean current of the ryanodol modified channel was ~47% of the control current. Ryanodol modifications lasted 3.8 ± 0.2 s and ryanodol action was Po dependent. The highest probability of action was during long open events. Unlike low doses of ryanodine [6], the presence of ryanodol did not increase the Po of unmodified RyR2 channels. Also, high doses of ryanodol did not fully close the channel as reported for high doses of ryanodine [6]. However, the low affinity of ryanodol-channel interaction (K_D ~40 μM) precluded its application at a comparably high dose (>1000 times the K_D). Lastly, the ryanodol action on channels was readily reversible upon ryanodol washout in contrast to the classical action of ryanodine on channels.

The action of ryanodol reported here on single RyR2 channels is quite consistent with previous reports [37, 38]. Like previous studies, we observed excess noise in the ryanoid modified state. The likely explanation for this increased noise is that the ryanodol modify

state is a collection of rapid transitions between two ryanodol-evoked pore conformations with slightly different ion-handling properties [37]. These two ryanoid-evoked pore conformations are most evident at membrane potentials >40 mV. Since the SR membrane potential in cells rarely (if ever) strays far from 0 mV [18], these conformations were not explored further here. Interestingly, Sigilas et al. [33] recently explored RyR2 modulation by calmodulin using ryanodol as a functional probe. Consistent with our study, they report that ryanodol acts primarily on open channels but they demonstrated that calmodulin modulates the ryanoid-channel association rate as well as the gating between the two ryanodol-evoked pore conformations. We found no indication that the Po sensitivity of ryanodol binding depended on how the channel was activated (via cytosolic Ca^{2+}, ATP or caffeine). We did not, however, test the action calmodulin which Sigilas et al. [33] reports is rather unique and may explain the discrepancy between calmodulin actions on ryanodine binding and single channel Po.

Ryanodol Action on Ca^{2+} Sparks

The amount of Ca^{2+} released during a Ca^{2+} spark is determined by the number of open RyR2 channels at a release site, the unit RyR2 Ca^{2+} current and the Po of the active channels. When ryanodol is applied near the K_D (as it was here), one might expect that ~50% of open RyR2 channels will be ryanodol modified. Ryanodol, however, preferentially binds during long opening which in cells (even during a spark) represent a fraction all the RyR2 openings. Thus, our results suggest that ryanodol binds to small subset of channels during a spark because ryanodol-evoked embers or glows [22, 44] were rarely observed. Say 10 channels are active during a Ca^{2+} spark and 3 of these channels become ryanodol modified. If these modified channels conduct ~50% of the control current, then the overall Ca^{2+} flux carried by the 10 open channels (7 unmodified) would be reduced by 15% (compared to 10 unmodified channels). Our Ca^{2+} spark results show that ryanodol reduced average Ca^{2+} spark amplitude by ~15%. Another tenable explanation for the observed reduced spark amplitude is that ryanodol reduced the SR Ca^{2+} load and this is discussed more below.

We found that ryanodol significantly increased the frequency of Ca^{2+} sparks. It did so by significantly increasing the probability that a release site will generate repetitive Ca^{2+} sparks. Ryanodol did not change the number of sites generating Ca^{2+} sparks. In other words, overall spark frequency was higher not because more sites were sparking but because already active sites were producing repetitive Ca^{2+} sparks. This implies that ryanodol preferentially acts on active release sites (i.e. those with open RyR2 channels) and leaves quiescent sites largely untouched. Our single channel results indicate that on average an individual ryanodol modification will last 3.8 s. During this period, the modified channel(s) will mediate a sustained low level Ca^{2+} release at the release site. We propose that this low level release is what repeatedly retriggers sparks at the same site. This retriggering would then logically end when ryanodol dissociates. The ratio of the amplitude of the last and first spark in a ryanodol-evoked spark train is ~0.4 suggesting local SR Ca^{2+} load may be temporarily depleted during the ryanodol modification. How might this influence the global SR Ca^{2+} load? First, the number of active sites generating repetitive sparks is a relatively small fraction of the total number of release sites in the cell. Second, a ryanodol modified release site likely remains so temporarily (~3.8 s) before returning to its normal unmodified condition. Thus, ryanodol may reduce the local SR Ca^{2+} load at a few active sites, but this may not substantially alter the overall global Ca^{2+} load across the entire cell. We believe this is the case because ryanodol had no significant effect on the global SR Ca^{2+} load (accessed via caffeine evoked release) or on electrically stimulated global Ca^{2+} transients (see supplementary material).

Repetitive Ca^{2+} sparks are interesting because they provide a means to explore certain local regulatory mechanisms like spark restitution and refractoriness [12, 34]. Ryanodol is not the only agent that evokes repetitive Ca^{2+} sparks at release sites. Imperatoxin A and low doses of ryanodine are known to do the same [15, 34]. Imperatoxin A intermittently modifies single RyR2 channels to long-lived subconductance states [39]. Terentyev et al. [15], like us, suggest the toxin evokes repeated sparks because the sustained low level local Ca^{2+} release mediated by a toxin-modified channel retriggers sparks at the same release site. Low dose ryanodine (<50 nM) is thought to elevate single RyR2 Po without evoking a long-lived subconductance state [6] and 50 nM ryanodine is known to trigger repeated sparks in cells [34]. These repeated sparks have been attributed to increased local RyR2 Po and not to a sustained low level local Ca^{2+} release. Since ≥50 nM ryanodine can evoke long-lived sub-conductance states [6], we suggest that all three agents (Imperatoxin A, ryanodol & 50 nM ryanodine) are likely triggering repeated sparks by the same mechanism. Namely, a sustained low level local Ca^{2+} release by a drug modified channel(s) re-igniting sparks at the same release site.

Summary

Ryanodol is not commercially available and consequently the overwhelming majority of investigators who seek to use a ryanoid end up using ryanodine. Depending on its concentration, ryanodine may elevate Po, modify or completely block a RyR2 channel [6, 5]. Also, the dissociation rate of ryanodine is relatively slow making ryanodine in effect an irreversible probe in many channel/cell experiments. In contrast, ryanodol action is simple, a bimolecular reaction. Its action on channels and Ca^{2+} sparks is readily reversible and ryanodol can be easily generated in almost any laboratory. Thus, we propose that ryanodol is a convenient and practical alternative to ryanodine in many studies of RyR-mediated Ca^{2+} release in cells.

Supplementary Material

Refer to Web version on PubMed Central for supplementary material.

Acknowledgments

This work was supported by NIH Grants HL057832 & HL064210 to MF, HL071741 to JRF, GM078665 to JAC, and Agence Nationale de la Recherche Grants ANR-09-GENO-012 & ANR-09-GENO-034 to AMG.

REFERENCES

1. Baudet S, Hove-Madsen L, Bers DM. How to make and use calcium-specific mini- and microelectrodes. Methods Cell Biol. 1994; 40:93–113. [PubMed: 8201986]
2. Bénitah JP, Perrier E, Gómez AM, et al. Effects of aldosterone on transient outward K^+ current density in rat ventricular myocytes. J. Physiol. (Lond.). 2001; 537:151–160. [PubMed: 11711569]
3. Bers, D. Excitation-Contraction Coupling and Cardiac Contractile Force. Kluwer Academic Press; 2001.
4. Bidasee KR, Besch HR. Structure-function relationships among ryanodine derivatives. Pyridyl ryanodine definitively separates activation potency from high affinity. J. Biol. Chem. 1998; 273:12176–12186. [PubMed: 9575165]
5. Bidasee KR, Xu L, Meissner G, et al. Diketopyridylryanodine has three concentration-dependent effects on the cardiac calcium-release channel/ryanodine receptor. J. Biol. Chem. 2003; 278:14237–14248. [PubMed: 12566457]
6. Buck E, Zimanyi I, Abramson JJ, et al. Ryanodine stabilizes multiple conformational states of the skeletal muscle calcium release channel. J. Biol. Chem. 1992; 267:23560–23567. [PubMed: 1331089]

7. Bull R, Marengo JJ, Suárez-Isla BA, et al. Activation of calcium channels in sarcoplasmic reticulum from frog muscle by nanomolar concentrations of ryanodine. Biophys. J. 1989; 56:749–756. [PubMed: 2554991]
8. Cannell MB, Cheng H, Lederer WJ. The control of calcium release in heart muscle. Science. 1995; 268:1045–1049. [PubMed: 7754384]
9. Chamberlain BK, Fleischer S. Isolation of canine cardiac sarcoplasmic reticulum. Meth. Enzymol. 1988; 157:91–99. [PubMed: 3231096]
10. Cheng H, Song LS, Shirokova N, et al. Amplitude distribution of calcium sparks in confocal images: theory and studies with an automatic detection method. Biophys. J. 1999; 76:606–617. [PubMed: 9929467]
11. Cheng H, Lederer W, Cannell M. Calcium sparks: elementary events underlying excitation-contraction coupling in heart muscle. Science. 1993; 262:740–4. [PubMed: 8235594]
12. Cheng H, Lederer WJ. Calcium sparks. Physiol. Rev. 2008; 88:1491–1545. [PubMed: 18923188]
13. Cheng H, Wang S. Calcium signaling between sarcolemmal calcium channels and ryanodine receptors in heart cells. Front. Biosci. 2002; 7:d1867–1878. [PubMed: 12161336]
14. Chu A, Díaz-Muñoz M, Hawkes, et al. Ryanodine as a probe for the functional state of the skeletal muscle sarcoplasmic reticulum calcium release channel. Mol. Pharmacol. 1990; 37:735–741. [PubMed: 1692609]
15. Terentyev, Dmitry; Viatchenko-Karpinski, S.; Valdivia, HH., et al. Luminal Ca^{2+} controls termination and refractory behavior of Ca^{2+}-induced Ca^{2+} release in cardiac myocytes. Circ. Res. 2002; 91:414–420. [PubMed: 12215490]
16. Fernández-Velasco M, Rueda A, Rizzi N, et al. Increased Ca^{2+} sensitivity of the ryanodine receptor mutant RyR2R4496C underlies catecholaminergic polymorphic ventricular tachycardia. Circ. Res. 2009; 104:201–209. 12p following 209. [PubMed: 19096022]
17. Fill M, Copello J. Ryanodine receptor calcium release channels. Physiol Rev. 2002; 82:893–922. [PubMed: 12270947]
18. Gillespie D, Fill M. Intracellular calcium release channels mediate their own countercurrent: the ryanodine receptor case study. Biophys. J. 2008; 95:3706–3714. [PubMed: 18621826]
19. Gómez AM, Cheng H, Lederer WJ, et al. Ca^{2+} diffusion and sarcoplasmic reticulum transport both contribute to $[Ca^{2+}]$i decline during Ca^{2+} sparks in rat ventricular myocytes. J. Physiol. (Lond.). 1996; 496(Pt 2):575–581. [PubMed: 8910239]
20. Gómez AM, Rueda A, Sainte-Marie Y, et al. Mineralocorticoid modulation of cardiac ryanodine receptor activity is associated with downregulation of FK506-binding proteins. Circulation. 2009; 119:2179–2187. [PubMed: 19364981]
21. González A, Kirsch WG, Shirokova N, et al. The spark and its ember: separately gated local components of Ca^{2+} release in skeletal muscle. J. Gen. Physiol. 2000; 115:139–158. [PubMed: 10653893]
22. Hui CS, Besch HR, Bidasee KR. Effects of ryanoids on spontaneous and depolarization-evoked calcium release events in frog muscle. Biophys. J. 2004; 87:243–255. [PubMed: 15240461]
23. Humerickhouse RA, Bidasee KR, Gerzon K, et al. High affinity C10-Oeq ester derivatives of ryanodine. Activator-selective agonists of the sarcoplasmic reticulum calcium release channel. J. Biol. Chem. 1994; 269:30243–30253. [PubMed: 7982934]
24. Jenden DJ, Fairhurst AS. The pharmacology of ryanodine. Pharmacol. Rev. 1969; 21:1–25. [PubMed: 4887724]
25. Kirsch WG, Uttenweiler D, Fink RH. Spark- and ember-like elementary Ca^{2+} release events in skinned fibers of adult mammalian skeletal muscle. J. Physiol. (Lond.). 2001; 537:379–389. [PubMed: 11731572]
26. Lindsay AR, Tinker A, Williams AJ. How does ryanodine modify ion handling in the sheep cardiac sarcoplasmic reticulum Ca^{2+}-release channel? J. Gen. Physiol. 1994; 104:425–447. [PubMed: 7807056]
27. Lipp P, Niggli E. Modulation of Ca^{2+} release in cultured neonatal rat cardiac myocytes. Insight from subcellular release patterns revealed by confocal microscopy. Circ. Res. 1994; 74:979–990. [PubMed: 8156645]

28. López-López JR, Shacklock PS, Balke CW, et al. Local calcium transients triggered by single L-type calcium channel currents in cardiac cells. Science. 1995; 268:1042–1045. [PubMed: 7754383]
29. Lukyanenko V, Gyorke S. Ca^{2+} sparks and Ca^{2+} waves in saponin-permeabilized rat ventricular myocytes. J. Physiol. (Lond.). 1999; 521(Pt 3):575–585. [PubMed: 10601490]
30. Pereira L, Métrich M, Fernández-Velasco M, et al. The cAMP binding protein Epac modulates Ca^{2+} sparks by a Ca^{2+}/calmodulin kinase signalling pathway in rat cardiac myocytes. J. Physiol. (Lond.). 2007; 583:685–694. [PubMed: 17599964]
31. Rousseau E, Smith JS, Meissner G. Ryanodine modifies conductance and gating behavior of single Ca^{2+} release channel. Am. J. Physiol. 1987; 253:C364–368. [PubMed: 2443015]
32. Shtifman A, Ward CW, Wang J, et al. Effects of imperatoxin A on local sarcoplasmic reticulum Ca^{2+} release in frog skeletal muscle. Biophys. J. 2000; 79:814–827. [PubMed: 10920014]
33. Sigalas C, Mayo-Martin MB, Jane DE, et al. Ca^{2+}-calmodulin increases RyR2 open probability yet reduces ryanoid association with RyR2. Biophys. J. 2009; 97:1907–1916. [PubMed: 19804721]
34. Sobie EA, Song L, Lederer WJ. Local recovery of Ca^{2+} release in rat ventricular myocytes. J. Physiol. (Lond.). 2005; 565:441–447. [PubMed: 15817631]
35. Tanna B, Welch W, Ruest L, et al. The interaction of a neutral ryanoid with the ryanodine receptor channel provides insights into the mechanisms by which ryanoid binding is modulated by voltage. J. Gen. Physiol. 2000; 116:1–9. [PubMed: 10871634]
36. Tanna B, Welch W, Ruest L, et al. Ryanoid modification of the cardiac muscle ryanodine receptor channel results in relocation of the tetraethylammonium binding site. J. Gen. Physiol. 2001; 117:385–394. [PubMed: 11331348]
37. Tanna B, Welch W, Ruest L, et al. Excess noise in modified conductance states following the interaction of ryanoids with cardiac ryanodine receptor channels. FEBS Lett. 2002; 516:35–39. [PubMed: 11959098]
38. Tinker A, Sutko JL, Ruest L, et al. Electrophysiological effects of ryanodine derivatives on the sheep cardiac sarcoplasmic reticulum calcium-release channel. Biophys. J. 1996; 70:2110–2119. [PubMed: 9172735]
39. Tripathy A, Resch W, Xu L, et al. Imperatoxin A induces subconductance states in Ca^{2+} release channels (ryanodine receptors) of cardiac and skeletal muscle. J. Gen. Physiol. 1998; 111:679–690. [PubMed: 9565405]
40. Tu Q, Velez P, CortesGutierrez M, et al. Surface charge potentiates conduction through the cardiac ryanodine receptor channel. J. Gen. Physiol. 1994; 103:853–867. [PubMed: 8035165]
41. Wang JP, Needleman DH, Hamilton SL. Relationship of low affinity $^{[3]}$ryanodine binding sites to high affinity sites on the skeletal muscle Ca^{2+} release channel. J. Biol. Chem. 1993; 268:20974–20982. [PubMed: 8407933]
42. Welch W, Ahmad S, Airey JA, et al. Structural determinants of high-affinity binding of ryanoids to the vertebrate skeletal muscle ryanodine receptor: a comparative molecular field analysis. Biochemistry. 1994; 33:6074–6085. [PubMed: 8193121]
43. Yellen G. Ionic permeation and blockade in Ca^{2+}-activated K^{+} channels of bovine chromaffin cells. J. Gen. Physiol. 1984; 84:157–186. [PubMed: 6092514]
44. Zhou J, Brum G, Gonzalez A, et al. Ca^{2+} sparks and embers of mammalian muscle. Properties of the sources. J. Gen. Physiol. 2003; 122:95–114. [PubMed: 12835473]

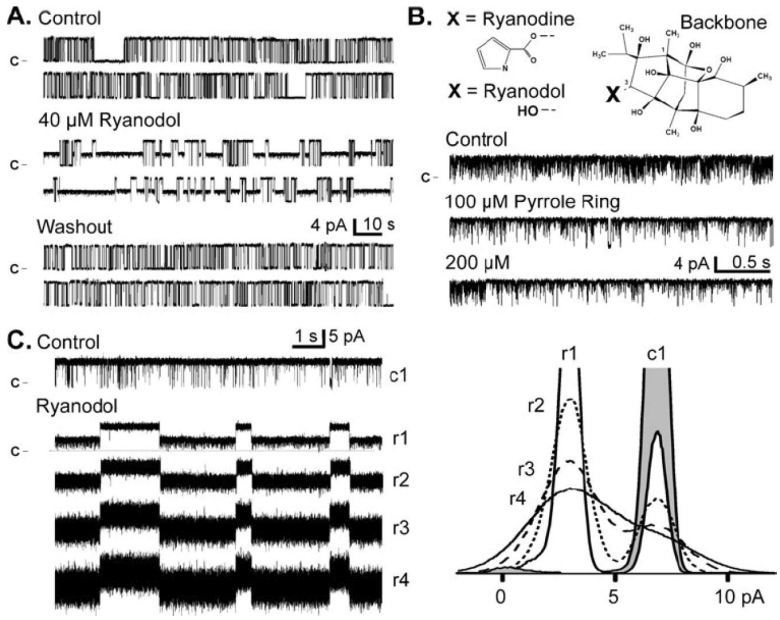

Fig. 1.

Ryanodol modifies single RyR2 function, Openings are upward deflections from the marked closed current level. **a** Ryanodol action is reversible. All data here are from the same single RyR2 channel recorded at 20 mV. Sample recordings in the *top panel* are in the absence of ryanodol (control). Sample recordings in the *central panel* are after 40 μM ryanodol was added to the cytosolic chamber. The *bottom panel* shows sample recordings after the cytosolic chamber solution was exchanged with a ryanodol-frce solution. The washout period was 5 min long during which 12 volume exchanges were completed. [b] The ryanoid backbone structure and the 3-C substitutions (X) that produce ryanodine (pyrrole ring) or ryanodol (hydroxyl) are shown (top). Sample single RyR2 channel recordings (*bottom*) are shown before (control) and after cytosolic addition of the pyrrole ring. **c** Sample single RyR2 channel recordings without (control) and with 40 μM ryanodol present are shown (*left*). Here, sample rate was 10 kHz, and trace numbering (c1, r1, r2, r3, and r4) indicates filtering level in kHz. At right are the corresponding all-points histograms (superimposed). The control histogram (c1) is shaded and ryanodol histograms (r1, r2, r3, and r4) are not

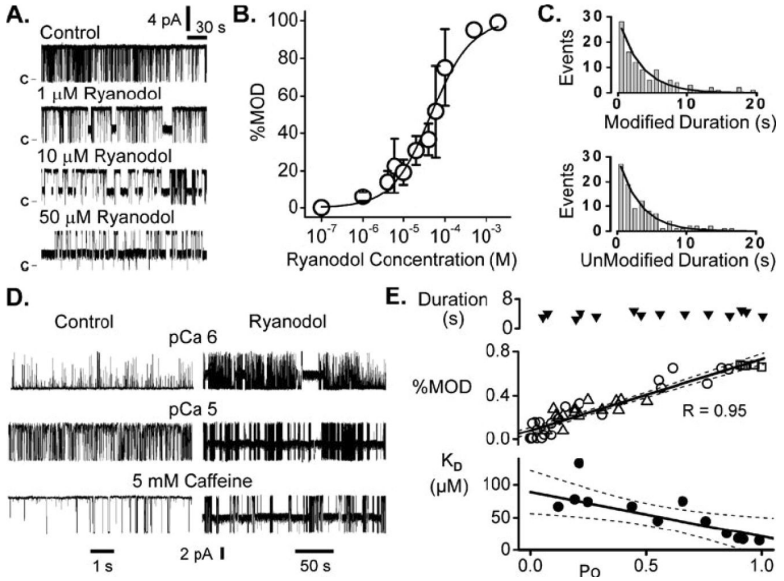

Fig. 2.

Ryanodol action is dose and open probability dependent. **a** Sample single RyR2 recordings in the absence (control) and presence of different ryanodol concentrations. Openings are upward deflections from marked closed current level. Recordings here were made a 20 mV. **b** Ryanodol dose–response plot revealing an EC_{50} of 46.4±6 μM. Points are means and SEM of three to eight determinations. **c** Histograms of the time spent in the ryanodol modified (*top*) or unmodified states (*bottom*). *Lines* are single exponential fits. **d** Ryanodol action at different RyR2 Po levels. Sample recordings at 20 mV from three different channels before (control) and after 40 μM ryanodol was added to the cytosolic solution. These channels were activated by cytosolic Ca^{2+} (1 or 10 μM) or caffeine. Records at left are time compressed to better show the ryanodol action. **e** Summary results from 14 different channels exploring the relationship between Po and ryanodol action. These data were obtained from RyR2 channels activated by cytosolic Ca^{2+} (1, 5, or 10 μM; *circles*), cytosolic ATP (0.5, 1, or 2 mM; *triangles*), or cytosolic caffeine (5 mM; *squares*) in the presence of 40 μM ryanodol. The Po was measured during the unmodified periods (i.e., with ryanodol present). The *top panel* shows ryanodol modification duration as a function of Po. The *center panel* shows how the percentage of time the channel spends in the ryanodol modified state (%MOD) varies with Po. The *bottom panel* shows how the ryanodol apparent K_D varies with Po. The K_D here was determined from ryanodol association and dissociation rates using Eq. 2. The dissociation and association rates were determined by fitting of ryanodol-modified and unmodified duration histograms (as illustrated by part **c**). *Thick solid lines* in the lower two panels are linear regressions. *Dotted lines* represent 95% confidence bands

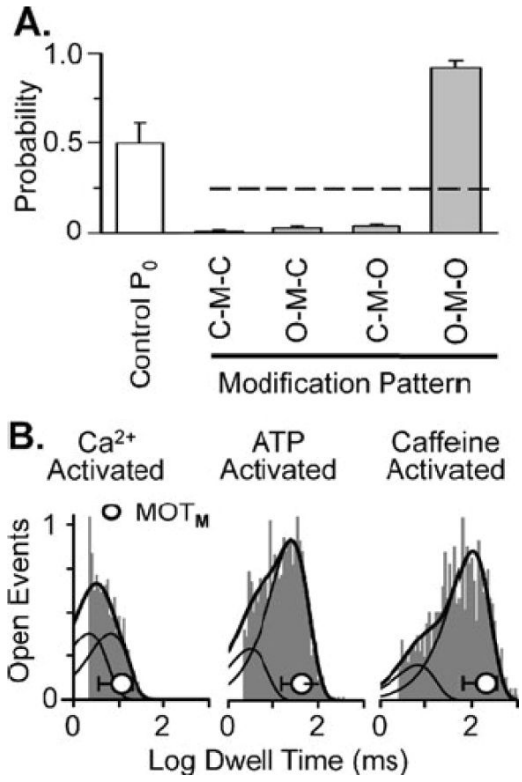

Fig. 3.

Ryanodol acts on open RyR2 channels. **a** Probability of different patterns of ryanodol modification. Individual ryanodol-modifications (*n*=385) from 22 different RyR2 channels were analyzed. These data were collected at 20 mV in the presence of 40 μM ryanodol. *Open bar* represents average Po during unmodified periods (0.49±0.11). Individual drug modification events were classified into four different categories (O–M–O, C–M–C, O–M–C, and C–M–O). The O refers to the fully open state. The C refers to the fully closed state. The M refers to the drug-modified state. The *dashed line* represents the 0.25 probability level. **b** Representative open dwell time histogram collected from a Ca^{2+}, an ATP, or a caffeine-activated channel. These data represent open dwell times to the fully open state during unmodified periods. Histograms were fit by two exponential components. *Solid cureve* represents the sum of the two components. The *dashed curves* represent the individual components. The mean open time of full conductance openings immediately preceding the ryanodol modification (MOT_M ± SD) in each case is superimposed on each histogram (*open circle*). For the Ca^{2+}-activated channel, τ_1 was 3.6 ms, τ_2 was 11.0 ms, and MOT_M was 11.4±7.9 ms. For the ATP-activatcd channel, τ_1 wras 7.3, τ_2 was 59.6 ms. and MOT_M was 43.7±28.0 ms. For the caffeine-activated channel, τ_1 was 16.2,τ_2 was 239.9 ms, and $M0T_M$ was 208.1±144.7 ms

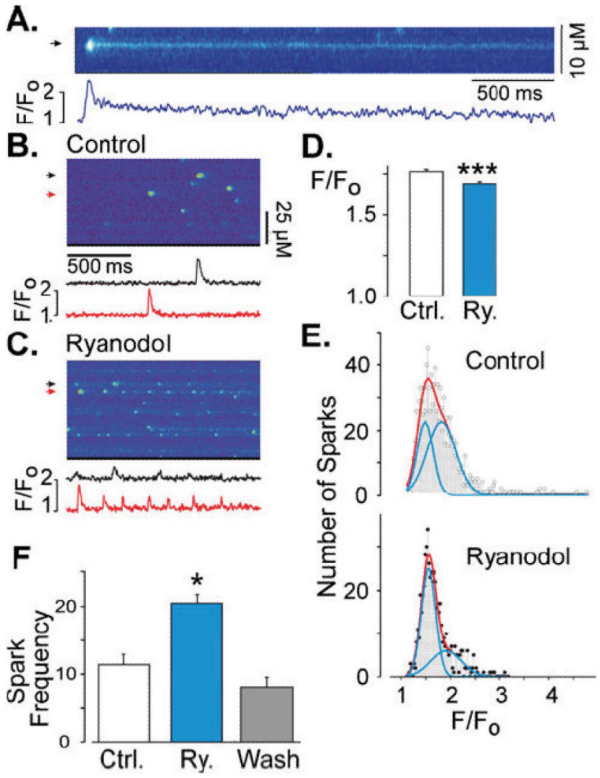

Fig. 4.

Ryanodol action on Ca^{2+} sparks in permeabilized myocytes. **a** Line scan image of a Ca^{2+} spark recorded in a permeabilized cardiac myocyte perfused with 10 μM ryanodine. Shown below is a fluorescence profile trace (F/FO; F = fluorescence signal, F0 = basal fluorescence) at the position marked by an *arrow*. **b** Control line scan image recorded in a permeabilized cell showing spontaneous Ca^{2+} sparks. Shown below are fluorescence profiles at the positions marked by the *color-coded arrows*. **c** Line scan image recorded from the same myocytc as in **b** but now during perfusion with 50 μM ryanodol. Again, fluorescence profiles are shown below. **d** Bar graph indicating the average Ca^{2+} spark amplitude recorded in control (*white bar*, n=1044 Ca^{2+} sparks, 12 cells) and after ryanodol treatment (*blue bar*, n=644 Ca^{2+} sparks, 9 cells). Triple asterisks indicate p<0.00.1. **e** Frequency histograms of Ca^{2+} spark amplitude (F/F0) recorded in control (top) and after ryanodol treatment (*bottom*). *Red lines* are double-Gauss fits. *Blue lines* are the individual Gauss functions. Fitting of the control histogram revealed peaks at 1.5 and 1.8 (F/F0), R=0.9387). Fitting of the ryanodol histogram revealed peaks at 1.55 and 1.9 (R=0.9471). This indicates that ryanodol decreased average spark amplitude by increasing the propoition of smaller amplitude Ca^{2+} sparks. Note that the control histogram could be well fit by a single-Gaussian function (R=0.971), but the ryanodol histogram was poorly fit by a single-Gaussian function (R=0.665). Thus, double-Gaussian fits were used in both cases. **f** Bar graph demonstrating the reversibility of ryanodol action on spark frequency. Single asterisk indicates p<0.05

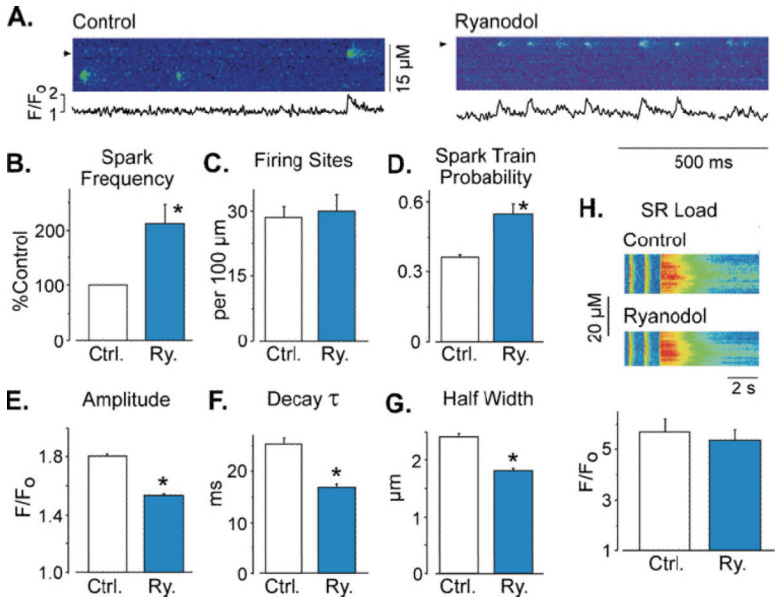

Fig. 5.

Ryanodol action on Ca^{2+} sparks in iniact myoeytes. An asterisk indicates $p<0.001$. **a** Line scan images showing Ca^{2+} sparks in before (left and center) and following 50 μM ryanodol application (right). Shown below are fluorescence profile traces (F/F0) at the positions marked by the *arrows*. **b** Ca^{2+} spark frequency (Ca^{2+} sparks per second per 100 μm line; n=4) determined in control cells before (*white bar*) and after 2-min lyanodol exposure (*blue bar*). **c** Number of sites that generate at least one Ca^{2+} spark during a 15-s recording period. **d** Probability that a site generates repeated Ca^{2+} sparks (i.e., a spark train). **e** Average of Ca^{2+} sparks amplitude in control (*white bar*, n=297 Ca^{2+} sparks in 14 cells) and after ryanodol exposure (*blue bar*, n=412 Ca^{2+} sparks. 9 cells). **f** Time constant of Ca^{2+} sparks decay (obtained by single exponential fitting of individual spark F/F0 decay). **g** Full width at half-maximal Ca^{2+} spark amplitude. **h** SR Ca^{2+} load obtained by rapid caffeine perfusion before (*white bar*) and after ryanodol exposure (*blue bar*). Ryanodol did not significantly alter global SR Ca^{2+} load